

Molecular Cancer Therapeutics



Studies on Mechanism of Action of Anticancer Peptides by Modulation of Hydrophobicity Within a Defined Structural Framework

Yi-bing Huang, Xiao-fei Wang, Hong-ye Wang, et al.

Mol Cancer Ther 2011;10:416-426. Published OnlineFirst January 20, 2011.

| | |
|-------------------------------|---|
| Updated version | Access the most recent version of this article at: doi:10.1158/1535-7163.MCT-10-0811 |
| Supplementary Material | Access the most recent supplemental material at: http://mct.aacrjournals.org/content/suppl/2011/01/21/1535-7163.MCT-10-0811.DC1.html |

| | |
|-----------------------|--|
| Cited Articles | This article cites by 27 articles, 7 of which you can access for free at: http://mct.aacrjournals.org/content/10/3/416.full.html#ref-list-1 |
|-----------------------|--|

| | |
|-----------------------------------|---|
| E-mail alerts | Sign up to receive free email-alerts related to this article or journal. |
| Reprints and Subscriptions | To order reprints of this article or to subscribe to the journal, contact the AACR Publications Department at pubs@aacr.org . |
| Permissions | To request permission to re-use all or part of this article, contact the AACR Publications Department at permissions@aacr.org . |

Studies on Mechanism of Action of Anticancer Peptides by Modulation of Hydrophobicity Within a Defined Structural Framework

Yi-bing Huang¹, Xiao-fei Wang¹, Hong-ye Wang¹, Yu Liu², and Yuxin Chen¹

Abstract

In the present study, the hydrophobicity of a 26-residue α -helical peptide (peptide P) was altered to study the effects of peptide hydrophobicity on the mechanism of action of cationic anticancer peptides. Hydrophobicity of the nonpolar face of the peptides was shown to correlate with peptide helicity. The self-association ability of peptides in aqueous environment, determined by the reversed-phase high performance liquid chromatography temperature profiling, showed strong influence on anticancer activity. The peptide analogues with greater hydrophobicity showed stronger anticancer activity determined by IC₅₀ values with a necrotic-like membrane disruption mechanism. Peptide analogues exhibited high specificity against cancer cells and much higher anticancer activity than widely-used anticancer chemical drugs. The mechanism of action of anticancer peptides was also investigated. The hydrophobicity of peptides plays a crucial role in the mechanism of action against cancer cells, which could present a way, using a *de novo* design approach, to create anticancer peptides as potential therapeutics in clinical practices. *Mol Cancer Ther*; 10(3); 416–26. ©2011 AACR

Introduction

Many natural or synthetic cationic peptides have been reported to show anticancer activity with characteristics including the ability to kill target cells rapidly, the broad spectrum of activity, and the specificity for cancer cells (1–2). Compared with the traditional cancer treatments such as chemotherapy or radioactive treatment, peptides with high specificity against cancer cells may present the way of killing cancer cells while protecting normal cells and helping patients to recover rapidly.

Of all the proposed mechanisms, 2 general effects of anticancer peptides against cancer cells were suggested: cytoplasmic membrane disruption via micellization or pore formation, and induction of apoptosis (3). In addition to these effects, some anticancer peptides have been reported to display anticancer activity via different mechanisms. Peptide buforin IIb targets cancer cells

through the interaction with cell surface gangliosides and induces mitochondria-dependent apoptosis (4). The peptide D-K₆L₉ exhibits selective cytotoxicity attributed to its electrostatic interaction with surface-exposed phosphatidylserine in cancer cells (5). Brevinin-2R activates the lysosomal-mitochondrial death pathway and involves autophagy-like cell death (6). From numerous structure/activity studies on both natural and synthetic anticancer peptides, a number of factors believed to be important for anticancer activity have been identified, including hydrophobicity, net charge, amphipathicity, secondary structure in membrane, and oligomerization ability (1, 7, 8). Among those factors, hydrophobicity should play an important role on anticancer activity due to the hydrophobic environment of cell membrane.

In our previous work, we described peptide V13K as an amphipathic α -helical antimicrobial peptide with strong antimicrobial activity against various Gram-positive and Gram-negative bacteria and negligible hemolytic activity against human red blood cells (9). We also found that V13K showed significant anticancer activity against varying cancer cells in our preliminary studies. In the present work, we use V13K (peptide P in this study) as the framework to modulate the peptide hydrophobicity on the nonpolar face of the helix, to investigate mechanism of action of peptides against cancer cells and to show the influence of hydrophobicity on anticancer effect. We report here that peptides use a rapid membrane-disruption mechanism to kill varying cancer cells and hydrophobicity plays a crucial role during the action, which is important for *de novo* designing anticancer peptides for clinical practices.

Authors' Affiliations: ¹Key Laboratory for Molecular Enzymology and Engineering of the Ministry of Education; and ²The Second Hospital, Jilin University, Changchun, Jilin, China

Note: Supplementary data for this article is available at Molecular Cancer Therapeutics Online (<http://mct.aacrjournals.org>).

Corresponding Authors: Yuxin Chen, Key Laboratory for Molecular Enzymology and Engineering of the Ministry of Education, Jilin University, Rm. 244, No. 3 Tang Ao-qing Bldg., 2699 Qianjin St., Changchun, Jilin, China 130012. Phone: 86-431-85155220; Fax: 86-431-85155200. E-mail: chen_yuxin@jlu.edu.cn; or Yu Liu, The Second Hospital of Jilin University, 218 Ziqiang Street, Changchun, Jilin, China 130041. Phone: 86-431-88796714; Fax: 86-431-88796794. E-mail: drliuy@jlu.edu.cn

doi: 10.1158/1535-7163.MCT-10-0811

©2011 American Association for Cancer Research.

Materials and Methods

Materials

Rink amide 4-methylbenzhydrylamine resin (MBHA resin; 0.8 mmol/g), all of the N - α -Fmoc protected amino acids and coupling reagents for peptide synthesis, trifluoroacetic acid (TFA) were purchased from GL Biochem. Other reagents such as Triton X-100, 5-fluorouracil, etoposide, fluorescein isothiocyanate (FITC), MTT, were all purchased from Sigma-Aldrich, Inc. FITC–Annexin V and Apoptosis Detection Kit I were from BD Biosciences. Acetonitrile (HPLC grade) was obtained from Fisher Scientific Worldwide Co. 2,2,2-Trifluoroethanol (TFE) was analytical grade and purchased from JinXin Chemicals.

Cell lines and cell culture

Human cervix carcinoma cells (HeLa), human melanoma cells (A375), human colorectal carcinoma cells (SW1116), human breast adenocarcinoma cells (MCF-7), human lung carcinoma cells (H1299), human rhabdomyosarcoma cells, human lung carcinoma cells (A549), and mouse melanoma cells (B16) were obtained from the American Type Culture Collection (ATCC) in 2010. ATCC does a series of procedures to characterize cell lines, including observations of morphologic appearance, iso-enzymology and/or the cytochrome *c* subunit I PCR assay for confirmation of species, short tandem repeat analyses to confirm human cell lines, and testing of antibody production and confirmation of the isotype for hybridoma cells. In this study, all cells were grown at 37°C in Dulbecco's modified Eagle's medium (DMEM) containing 100 U/mL penicillin, 100 µg/mL streptomycin and supplemented with 10% FBS (Invitrogen).

Peptide synthesis, FITC labeling, and purification

The peptides were synthesized by the solid-phase peptide synthesis using Fmoc (9-fluorenyl-methoxycarbonyl) chemistry as described previously (10). The labeling of the peptides with FITC was done as the methods described previously (11).

The crude peptides were purified by preparative Shimadzu LC-6A high-performance liquid chromatography (HPLC), using a Zorbax 300 SB-C₈ column (250 × 9.4-mm ID, 6.5-µm particle size, 300-Å pore size; Agilent Technologies) with a linear AB gradient (0.1% acetonitrile/min) at a flow rate of 2 mL/min, while eluent A was 0.1% aqueous TFA in water, and eluent B was 0.1% TFA in acetonitrile. The peptides were further characterized by mass spectrometry and amino acid analysis.

Analytical reversed-phase HPLC and temperature profiling of peptides

Peptide samples were analyzed on a Shimadzu LC-20A HPLC column. Runs were done on a Zorbax 300 SB-C₈ column (150 × 4.6-mm ID, 5-µm particle size, 300-Å pore size) from Agilent Technologies, using a linear AB gradient (1% acetonitrile/min) and a flow rate of 1 mL/min, in which eluent A was 0.1% aqueous TFA and eluent B

was 0.1% TFA in acetonitrile. Temperature profiling analyses during reversed phase (RP)-HPLC were done in 5°C increments, from 5°C to 80°C, as described previously (12, 13).

Circular dichroism spectroscopy

Circular dichroism spectra were acquired with a 0.02-cm path length quartz cuvette on a Jasco J-810 spectropolarimeter (Jasco) at 25°C as described previously (10). The concentration of 75 µmol/L peptides was measured in benign buffer (50 mmol/L KH₂PO₄/K₂HPO₄, 100 mmol/L KCl, pH 7) or benign buffer with 50% TFE at 25°C. The mean residue molar ellipticities were calculated by the equation $[\theta] = \theta/10lc_{MN}$ (9). The values of mean residue molar ellipticities of the peptide analogues at 222 nm were used to determine the relative helicity of the peptides.

In vitro cytotoxicity assays

The MTT assay has been used to test cytotoxicity of reagents and cell viability. Cells (5×10^3 to 1×10^4) were seeded in 96-well plates and incubated with serially 2-fold diluted concentrations of different peptides (0.6–86 µmol/L) for 36 hours at 37°C. As a negative control, cells were cultured without addition of the peptides. The well-used anticancer chemical drugs, 5-fluorouracil and etoposide, were also added to cells as positive controls. Thereafter, 200 µL of 5 mg/mL MTT solution in PBS was added to the cells and treated for 4 hours at 37°C. The formazan crystals were dissolved by adding 150 µL dimethyl sulfoxide just before spectrometric determination. The absorbance was determined at 490 nm. The results were expressed as IC₅₀, representing the concentration at which cell viability was reduced by 50%. The cytotoxicity assays were repeated in triplicates.

Measurement of hemolytic activity

Peptide samples were serially diluted by PBS in 96-well plates (round bottom) to give a volume of 60 µL sample solution in each well. Human erythrocytes anticoagulated by EDTAK were collected by centrifugation (1,000 × g) for 5 minutes, and washed twice by PBS, then diluted to a concentration of 2% in PBS. 60 µL of 2% erythrocytes were added to each well to give a final concentration of 1% human erythrocytes in each well and plates were incubated at 37°C for 1 hour. The plates were then centrifuged for 10 minutes at 3,000 rpm and supernatant (80 µL) was transferred to a 96-well plate (flat bottom). The release of hemoglobin was determined by measuring the absorbance of the supernatant at 540 nm. The hemolytic activity was determined as the minimal peptide concentration that caused hemolysis (minimal hemolytic concentration, MHC). Erythrocytes in PBS and distilled water were used as control of 0% and 100% hemolysis, respectively.

Confocal fluorescence microscopic studies

Confocal images were obtained using an Olympus Fluoview 1000 confocal laser scanning microscope.

Briefly, HeLa cells (4×10^5) were cultured in 6-well plate. After being treated with test samples and harvested, the cells were dyed with FITC–Annexin V/propidium iodide (PI) kit. The stained cells were centrifuged at 1,000 rpm for 5 minutes, and the cell pellets were dropped on sterile coverslips and then examined by fluorescence microscopy. For peptide-cell binding study, the FITC-labeled peptide (2 $\mu\text{mol/L}$ in PBS) was added to the cells grown on a 24-well plate, and a series of images were taken at different time intervals to study the changes of peptide binding and cell lysis.

Scanning electron microscopy

Sterilized coverslips were placed in the bottom of a 12-well plate. At least 3×10^4 cells were seeded in each well in 2 mL DMEM medium. The plates were incubated overnight under the same conditions as described before. The peptide (final concentration, 2 $\mu\text{mol/L}$) A12L/A20L was added the next day and the plate was incubated at 37°C for 1 hour. The medium containing A12L/A20L was then removed and subsequently 2 mL 2.5% glutaraldehyde solution (Sigma-Aldrich, in 0.1 mol/L phosphate buffer) was added to each well for 3 hours. After immediate fixation in glutaraldehyde, all coverslips were washed with 0.1 mol/L phosphate buffer at 4°C. Counterfixation in 2% osmium tetroxide (Sigma-Aldrich) for 2 hours was followed by dehydration in ethanol and drying in a critical point dryer. Cells on coverslips were coated with gold and analyzed by using a scanning electron microscope (JSM-5600; JEOL).

Results

Peptide design

The parent peptide (peptide P), also known as peptide V13K in our previous work (9), is a 26-residue amphipathic peptide which adopts an α -helical conformation in a hydrophobic environment (Fig. 1). In the present study, we used peptide P as a framework to systematically alter peptide hydrophobicity on the nonpolar face of the helix by replacing alanine residues with the more hydrophobic leucine residues to increase hydrophobicity or by changing leucine residues to alanine residues to decrease hydrophobicity. Figure 1 shows the peptide analogues represented as helical nets. To increase the hydrophobicity of peptide P, we choose the alanine to leucine substitution at position 12 (A12L) or 20 (A20L) as single Leu-substituted peptides. By introducing Leu at positions 12 and 20, we made double and triple Leu-substituted peptides (A12L/A20L and A12L/A20L/A23L) to further increase peptide hydrophobicity. In contrast, to decrease the hydrophobicity of peptide P, leucine was replaced by alanine at position 6 (L6A), 17 (L17A), or 21 (L21A) for single Ala-substituted peptides. Two double Ala-substituted peptides (L6A/L17A and L17A/L21A) were also used to further decrease the peptide hydrophobicity. The $i \rightarrow i + 3$ and $i \rightarrow i + 4$ hydrophobic interactions among large hydrophobes such as leucine residues stabilize the

α -helical structure, as shown in Fig. 1A. An 18-mer control peptide (peptide C; Ac-ELEKGGLEGEKGGKELEK-amide) was used for temperature profiling during RP-HPLC to monitor peptide self-association ability as described previously (9, 12, 13).

Peptide secondary structure

To show the effect of amino acid substitutions on peptide secondary structure, circular dichroism spectra of the peptide analogues were measured under benign conditions (50 mmol/L KH₂PO₄/K₂HPO₄, 100 mmol/L KCl, pH 7, referred to as KP buffer) and also in 50% TFE to mimic the hydrophobic environment of the membrane (Supplementary Fig. S1). Table 1 shows the molar ellipticity values at different environments and the helicity of peptide analogues relative to that of peptide A12L/A20L/A23L in the presence of 50% TFE ($[\theta]_{222} = -34,350$), which is the greatest value among all analogues. It is clear that in KP buffer, Ala-substituted peptides showed negligible helical structures with molar ellipticity values ranging from -1,450 to -2,700; Leu-substituted peptides exhibited different degrees of helical structure in aqueous environment with molar ellipticity values ranging from -4,300 to -16,900. In contrast, in the presence of 50% TFE, a mimic of the membrane's hydrophobic environment, high helical structure of almost all peptide analogues could be induced. It is clear that both under benign conditions and in the presence of 50% TFE, the relative helicities of the peptides are in the order L6A/L17A < L17A/L21A < L17A < L6A < L21A < P < A12L < A20L < A12L/A20L < A12L/A20L/A23L (Table 1).

Peptide hydrophobicity

The hydrophobicity of peptides was determined by measuring RP-HPLC retention behaviors, which are highly sensitive to the conformational status of peptides upon interaction with the hydrophobic environment of the column matrix (14, 15). In this study, the hydrophobicity at 5°C and 80°C of peptide analogues is shown in Table 1. Indeed, peptide hydrophobicity was changed in 2 ways, the difference of intrinsic hydrophobicity of side chains of substituting amino acids (16) and the alteration of the number of the $i \rightarrow i + 3$ and $i \rightarrow i + 4$ hydrophobic interactions of large hydrophobes which affects the continuity of the hydrophobic face of the peptide (17). Between these two factors, the hydrophobicity of amino acid side chains may play a more important role in changing peptide overall hydrophobicity in this study. The hydrophobicity of peptides (as expressed by RP-HPLC retention time t_R) is in the order of L6A/L17A < L17A/L21A < L17A < L21A < L6A < P < A12L < A20L < A12L/A20L < A12L/A20L/A23L (t_R ranging from 32.59 to 47.25 minutes at pH 2 and 5°C, Table 1). The $i \rightarrow i + 3$ and $i \rightarrow i + 4$ interactions among large hydrophobes such as leucine residues, which stabilize the α -helical structure in α -helical peptides, were shown in Fig. 1. Smaller

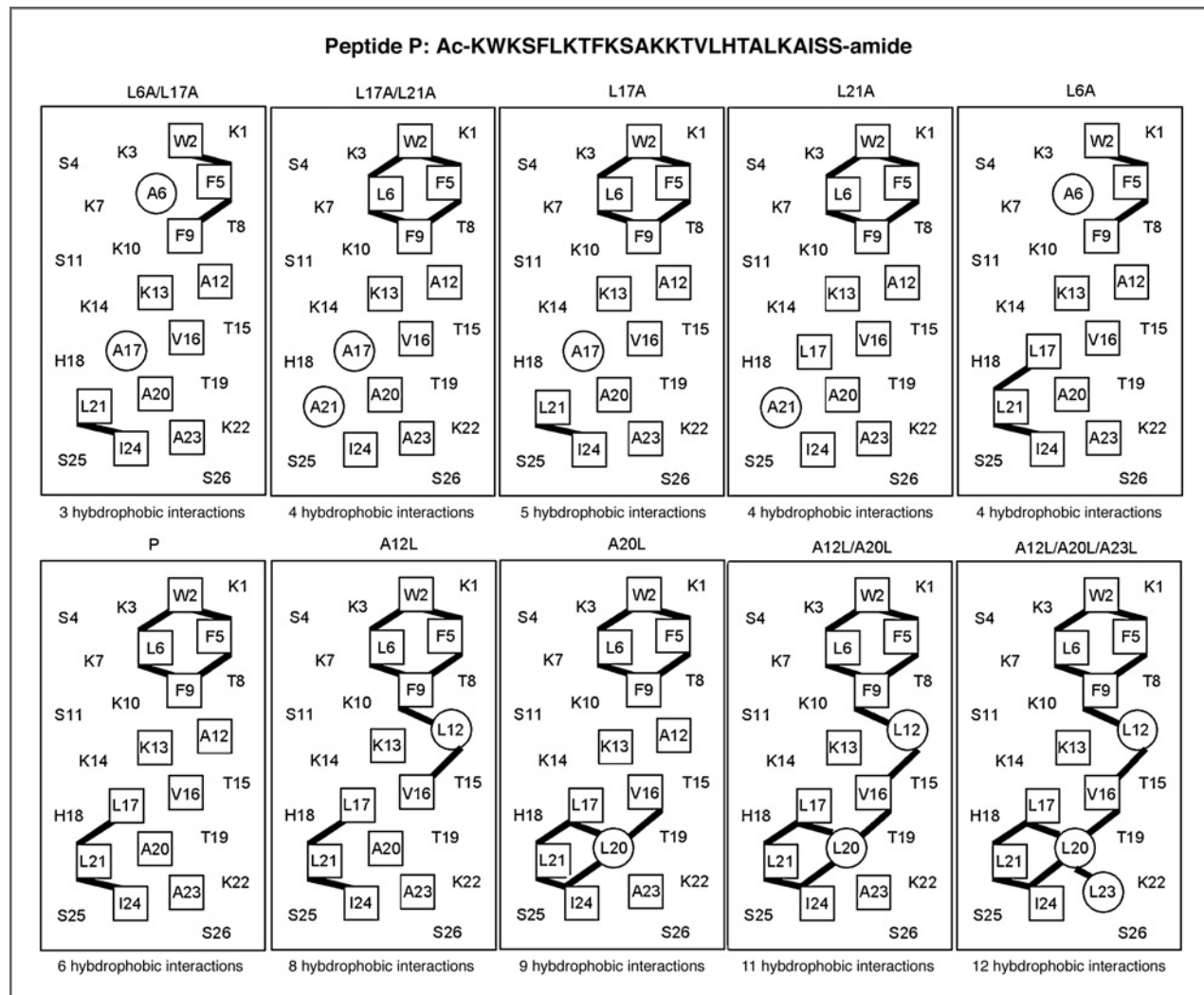


Figure 1. Helical net representation of the peptides. The amino acid residues on the nonpolar faces are boxed, and the substituting hydrophobic amino acid residues are circled. The $i \rightarrow i + 3$ and $i \rightarrow i + 4$ hydrophobic interactions are shown as black bars.

hydrophobic amino acid such as alanine usually does not involve in the $i \rightarrow i + 3$ and $i \rightarrow i + 4$ hydrophobic interactions because its short side-chain arm cannot reach the side chains of the neighboring amino acids at the $i \rightarrow i + 3$ and $i \rightarrow i + 4$ positions. The number of the $i \rightarrow i + 3$ and $i \rightarrow i + 4$ hydrophobic interactions on the nonpolar face of the helical peptides generally correlates with the observed hydrophobicity of the peptides, except for peptide L17A. Although peptides L17A, L21A, and L6A have single Ala substitution, L17A has more hydrophobic interactions but less observed hydrophobicity than the other two, which indicates that central location amino acid substitution on the nonpolar face of the peptide shows stronger influence on hydrophobicity.

Peptide self-association

As shown in Table 1, the ability of peptides to self-associate was determined by RP-HPLC temperature pro-

filing. Control peptide C is a monomeric random coil peptide in both aqueous and hydrophobic media; thus, its retention behavior within the temperature range of 5°C to 80°C represents only the general effects of temperature (18). After normalized with peptide C to eliminate the general temperature effects, the maximal values of the change of retention times during temperature change (Supplementary Fig. S1C) were defined as the peptide association parameter (P_A) to quantify the self-association ability of peptides in solution (Table 1). The details of how to determine peptide association parameter (P_A) were reported previously (9, 12, 13). As seen from the data in Table 1, peptide association parameter (P_A) is not correlated with peptide relative hydrophobicity during RP-HPLC (t_R), especially for the Ala-substituted peptide analogues. In this study, peptide self-association ability was correlated with peptide helicity in aqueous environment as measured by circular dichroism data in benign

Table 1. Biophysical data of the peptide analogues

| No. | Peptides ^a | Benign ^b | | 50% TFE ^c | | <i>t</i> _R ^e , min | | <i>P</i> _A ^f , min |
|-----|-----------------------|---------------------|----------------------|----------------------|----------------------|--|-------|--|
| | | [θ] ₂₂₂ | % helix ^d | [θ] ₂₂₂ | % helix ^d | 5°C | 80°C | |
| 1 | L6A/L17A | -1,450 | 4.2 | -17,600 | 51.2 | 32.59 | 30.12 | 0.47 |
| 2 | L17A/L21A | -1,700 | 4.9 | -19,900 | 57.9 | 33.16 | 30.94 | 0.55 |
| 3 | L17A | -2,350 | 6.8 | -22,000 | 64.0 | 34.76 | 32.75 | 0.81 |
| 4 | L21A | -2,700 | 7.9 | -24,600 | 71.6 | 35.66 | 33.49 | 0.68 |
| 5 | L6A | -2,450 | 7.1 | -22,700 | 66.1 | 35.75 | 33.37 | 0.56 |
| 6 | P | -3,400 | 9.9 | -26,400 | 76.9 | 38.02 | 36.10 | 0.93 |
| 7 | A12L | -4,300 | 12.5 | -31,900 | 92.9 | 41.64 | 40.52 | 1.65 |
| 8 | A20L | -4,700 | 13.7 | -32,500 | 94.6 | 42.59 | 41.35 | 1.63 |
| 9 | A12L/A20L | -10,500 | 30.6 | -33,000 | 96.1 | 45.75 | 46.21 | 3.42 |
| 10 | A12LA20LA23L | -16,900 | 49.2 | -34,350 | 100.0 | 47.25 | 50.61 | 7.04 |
| | C ^g | | | | | 22.56 | 19.91 | |

^aPeptides are ordered by relative hydrophobicity during RP-HPLC at 5°C.

^bThe mean residue molar ellipticities, [θ]₂₂₂ (degree·cm²/dmol) at wavelength 222 nm were measured at 25°C in KP buffer (100 mmol/L KCl, 50 mol/L PO₄, pH 7.0).

^cThe mean residue molar ellipticities, [θ]₂₂₂ (degree·cm²/dmol) at wavelength 222 nm were measured at 25°C in KP buffer diluted 1:1 (v/v) with TFE.

^dThe helical content (in percentage) of a peptide relative to the molar ellipticity value of peptide A12L/A20L/A23L in 50% TFE.

^e*t*_R (min.) denotes the retention time at 5°C and 80°C during the RP-HPLC temperature profiling.

^f*P*_A denotes the self-association parameter of each peptide during the RP-HPLC temperature profiling, which is the maximal retention time difference of [(*t*_R^t - *t*_R⁵ for peptide analogues) - (*t*_R^t - *t*_R⁵ for control peptide C)] within the temperature range, and (*t*_R^t - *t*_R⁵) is the retention time difference of a peptide at a specific temperature (t) compared with that at 5°C.

^gPeptide C is a random coil control used to calculate *P*_A values.

(KP buffer) as shown in Table 1. Peptide exhibited stronger helical structure in solution, showed better shape of the nonpolar face, and presented stronger ability to dimerize because dimers are formed by the interaction of the nonpolar faces of 2 peptide molecules.

Anticancer activity

The anticancer activities of the peptide analogues against various cancer cell lines are shown in Table 2. The geometric mean IC₅₀ values for 8 cancer cell lines were calculated to provide an overall evaluation of the anticancer activity of the peptide analogues after incubating with cancer cells for 36 hours. The Ala-substituted peptides showed weaker anticancer activity than that of the parent peptide P; in contrast, the Leu-substituted peptides exhibited greater anticancer activity against cancer cells on IC₅₀ values than peptide P. It is obvious that peptide hydrophobicity is correlated with anticancer activity; thus, increasing hydrophobicity leads to the increase of anticancer activity against different cancer cells.

Table 2 provides comparison of anticancer activities of peptides against HeLa cells with different treatment times and activities of well-used anticancer chemical drugs 5-fluorouracil and etoposide. It is surprising to see that there was no significant difference on anticancer activity of the peptides after incubating with cancer cells for 1 hour or 36 hours, respectively. This

phenomenon may represent the high killing propensity of anticancer peptides against different cancer cells; however, slightly higher IC₅₀ values of the peptides at 36 hours may be attributed to the propagation of surviving cells during longer incubation time. In contrast, 5-fluorouracil showed no detectable anti-HeLa activity at a concentration of 3,000 μmol/L after a 1-hour treatment and poor anti-HeLa activity with IC₅₀ value of 353.6 μmol/L after a 36-hour treatment, respectively. In addition, etoposide presented IC₅₀ values of 31.7 and 680 μmol/L against HeLa cell line for 36 hours and 1 hour, respectively. Among the peptide analogues tested, peptide A12L/A20L showed the strongest activity against HeLa cell line with the IC₅₀ value of 2 and 1.2 μmol/L at 36 hours and 1 hour, respectively. Because HeLa cell line was sensitive to the peptide analogues and easy to be handled during cell culture experiments, we chose HeLa as the target cell line for further mechanism study, whereas the peptide A12L/A20L as the attacking peptide.

Hemolytic activity

The MHC of the peptide analogues against human erythrocytes was determined as a major measure of peptide toxicity toward normal cells (Table 2). In this study, by substituting alanine on the nonpolar face of the helix, we improved the peptide hemolytic activity significantly up

Table 2. Anticancer (IC_{50}) and hemolytic (MHC) activities of peptide analogues, 5-fluorouracil and etoposide, against cancer cells and human red blood cells

| Peptides ^a | 36 h | | | | | | 1 h | | MHC ^d , μmol/L | Therapeutic index ^e |
|-----------------------------|-------------|-------------|-------------|-------------|-------------|-------------|-------------|-------------|------------------------------|-----------------------------------|
| | A549 | A375 | Mcf-7 | SW1116 | RD | H1299 | B16 | HeLa | GM ^c | HeLa |
| L6A/L17A | >83.6 | >83.6 | >83.6 | >83.6 | >83.6 | >83.6 | >83.6 | >83.6 | >83.6 | >334.4 |
| L17A/L21A | >83.6 | >83.6 | >83.6 | >83.6 | >83.6 | 37.7 ± 0.10 | >83.6 | >83.6 | >83.6 | >334.4 |
| L17A | >83.6 | >83.6 | >83.6 | >83.6 | >83.6 | 16.4 ± 0.06 | >83.6 | >83.6 | >83.6 | >334.4 |
| L21A | 71.0 ± 0.19 | 59.8 ± 0.15 | 70.8 ± 0.18 | >83.6 | >83.6 | 15.6 ± 0.05 | 63.5 ± 0.15 | 64.7 ± 0.15 | 51.8 | 44.5 ± 0.12 |
| L6A | 53.1 ± 0.06 | 58.7 ± 0.08 | 62.3 ± 0.08 | >83.6 | >83.6 | 14.0 ± 0.02 | 62.6 ± 0.07 | 58.6 ± 0.07 | 46.4 | 36.8 ± 0.04 |
| P | 33.1 ± 1.17 | 17.8 ± 0.62 | 15.8 ± 0.54 | 11.1 ± 0.37 | 25.2 ± 0.84 | 4.7 ± 0.16 | 11.5 ± 0.40 | 10.4 ± 0.37 | 14.0 | 10.6 ± 0.35 |
| A12L | 11.1 ± 0.08 | 4.3 ± 0.04 | 5.0 ± 0.03 | 6.4 ± 0.03 | 7.5 ± 0.04 | 4.4 ± 0.03 | 5.2 ± 0.04 | 3.8 ± 0.03 | 5.6 | 2.0 ± 0.01 |
| A20L | 8.7 ± 0.05 | 6.5 ± 0.03 | 5.1 ± 0.02 | 5.0 ± 0.05 | 9.8 ± 0.05 | 2.9 ± 0.05 | 7.8 ± 0.03 | 4.3 ± 0.03 | 5.9 | 1.7 ± 0.01 |
| A12L/A20L | 9.7 ± 0.24 | 8.7 ± 0.20 | 6.2 ± 0.13 | 4.3 ± 0.08 | 6.4 ± 0.16 | 4.1 ± 0.10 | 4.4 ± 0.12 | 2.0 ± 0.05 | 5.2 | 1.2 ± 0.02 |
| A12L/A20L/A23L | 9.2 ± 0.13 | 7.2 ± 0.12 | 5.7 ± 0.07 | 3.5 ± 0.06 | 5.5 ± 0.07 | 2.7 ± 0.38 | 4.6 ± 0.07 | 2.2 ± 0.02 | 4.6 | 1.9 ± 0.03 |
| 5-fluorouracil ^f | ND | 353.6 ± 1.81 | 2.6 ± 0.01 |
| etoposide ^f | ND | >3,000 | 1.4 |
| | | | | | | 31.7 ± 0.14 | ND | ND | >680 | >334.4 |

Abbreviations: RD, human rhabdomyosarcoma cells; ND, data not determined.

^aPeptides are ordered by relative hydrophobicity during RP-HPLC at 5°C.^bAnticancer activity (IC_{50}) represents the concentration of peptides at which cell viability was reduced by 50% in comparison to untreated cells. The MTT assay was repeated in triplicate and IC_{50} value was determined by averaging 3 repeated experiments.^cGM, geometric mean of the anticancer activity (IC_{50}) for the 8 cancer cell lines, represents the overall anticancer activity of different peptides after incubating with cancer cells for 36 hours.^dHemolytic activity (MHC) was determined on human red blood cells after incubating with peptides for 1 hour (hRBC).^eTherapeutic index, MHC/ IC_{50} , the values of IC_{50} used for the calculation were from data of 1 hour. Larger values indicate greater anticancer specificity.^f5-fluorouracil and etoposide were used to treat HeLa for 36 hours and 1 hour.

to no detectable hemolysis at the concentration of 334.4 $\mu\text{mol/L}$. However, the Leu-substituted peptides with enhanced hydrophobicity exhibited stronger hemolytic activity than peptide P, from 41.8 $\mu\text{mol/L}$ for A12L to 2.6 $\mu\text{mol/L}$ for A12L/A20L/A23L, which were 4-fold to 64.3-fold increases in hemolysis compared with that of the peptide P, respectively. From Table 2, it is clear that similar to anticancer activity, hemolytic activity was correlated with peptide hydrophobicity as well, although within different magnitude, that is, the greater the hydrophobicity of peptides, the stronger the hemolysis against human red blood cells. Two chemical drugs etoposide and 5-fluorouracil showed no hemolysis at the concentrations of 334.4 $\mu\text{mol/L}$.

Peptide specificity (therapeutic index)

The therapeutic index is a widely used parameter to represent the specificity of potential reagents. It is calculated by the ratio of MHC (hemolytic activity) and IC_{50} (anticancer activity); thus, larger values in therapeutic index indicate greater anticancer specificity. In this study, we took HeLa cell line as an example to calculate peptide therapeutic index. In Table 2, compared with the parent peptide P, the therapeutic indices of peptides against HeLa are increased with the increase of hydrophobicity from 15.8 to 24.6 (from peptide P to A20L) and are decreased with further increase in hydrophobicity from 24.6 to 1.4 (from A20L to A12L/A20L/A23L), respectively. The peptide A20L exhibits the highest therapeutic index of 24.6 among the peptides, representing that the anti-HeLa activity of peptide A20L is 24.6-fold greater than its toxicity against human red blood cells. Compared with the anticancer peptides, etoposide and 5-fluorouracil exhibited low therapeutic index values due to the low anticancer activities.

Membrane binding and disruption of anticancer peptide

To understand the mechanism of anticancer peptide interacting with the cancer cells, the time profiles of FITC-labeled peptide A12L/A20L interacting with HeLa cells at the concentration of its IC_{50} value were monitored by confocal fluorescence microscopy, as shown in Supplementary Figs. S2A–S2D. Peptide molecules were evenly distributed as green materials in the sight field at time zero, compared with the control (only cells without adding peptide). With longer interaction time, it is clear that the peptide bound strongly and rapidly on the surface of the cells. At the time of 20 minutes, almost all the peptide bound onto the cancer cells were shown as high-density bright green.

We used confocal fluorescence microscopy to explore the mode of action of peptide A12L/A20L with membrane by FITC–Annexin V/PI double staining (Fig. 2A–D). The HeLa cells with PBS as a negative control showed round and intact morphology with no dye staining (Fig. 2D). The apoptosis model, in which cells treated with etoposide (100 $\mu\text{g/mL}$) for 24 hours, exhib-

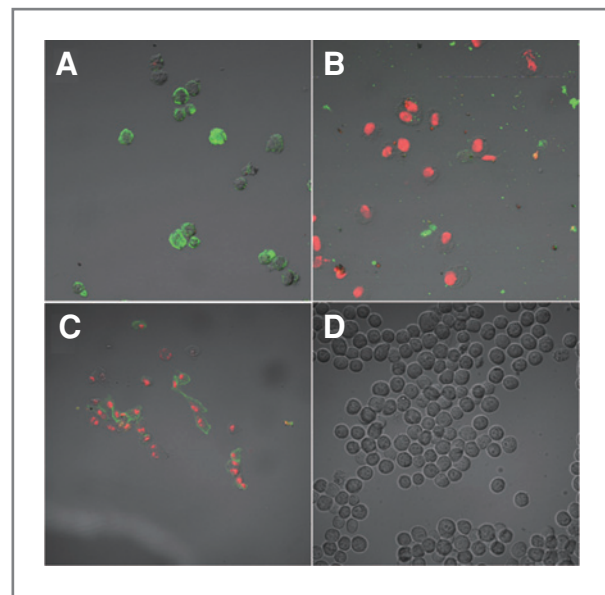


Figure 2. A-D, FITC–Annexin V/PI double staining assay of peptide A12L/A20L interacting with HeLa cells, using confocal fluorescence microscopy. D, untreated HeLa cells as control; A-C, treated images of HeLa cells; the treated time was 24 hours for anticancer chemical drug etoposide (A); 1 hour for anticancer peptide A12L/A20L (B); and 1 hour for Triton X-100 (C), respectively. Green, cell membrane dyed by Annexin V; red, nuclei dyed by PI reagent. All images from A-D are in $\times 400$ magnification.

ited early apoptosis with FITC–Annexin V-positive (green) and PI-negative staining (Fig. 2A). The diluted Triton X-100 (200 $\mu\text{mol/L}$) treated cells for 1 hour were used as the positive control of acute necrosis (8). The cells treated with Triton X-100 exhibited disrupted membrane with FITC–Annexin V binding and PI incorporation or PI staining only (red; Fig. 2C). It is strange to see that cells treated with Triton X-100 showed shrunk or disrupted morphology of nucleus. After treating with A12L/A20L (2 $\mu\text{mol/L}$) for 1 hour, cells remained round shape with PI-stained nucleus in red and minor FITC–Annexin V binding on cell membrane (Fig. 2B), which indicates that anticancer peptide disrupted cell membrane of cancer cells in a necrosis-like way and allowed PI to enter the cytoplasm and dye the nucleus.

Scanning electron microscopy

The subtle morphologic changes on the HeLa cell membrane with or without peptide A12L/A20L treatment were examined by scanning electron microscopy. As shown in Fig. 3, cell surface was examined at $\times 1,000$ and $\times 5,000$ magnification. The untreated HeLa cells showed plenty of microvilli and adherent smooth surface (Fig. 3A and B). In contrast, HeLa cells treated with peptide A12L/A20L revealed disrupted cell membrane with significant cavity formation and loss of microvilli and membrane integrity (Fig. 3C and D).

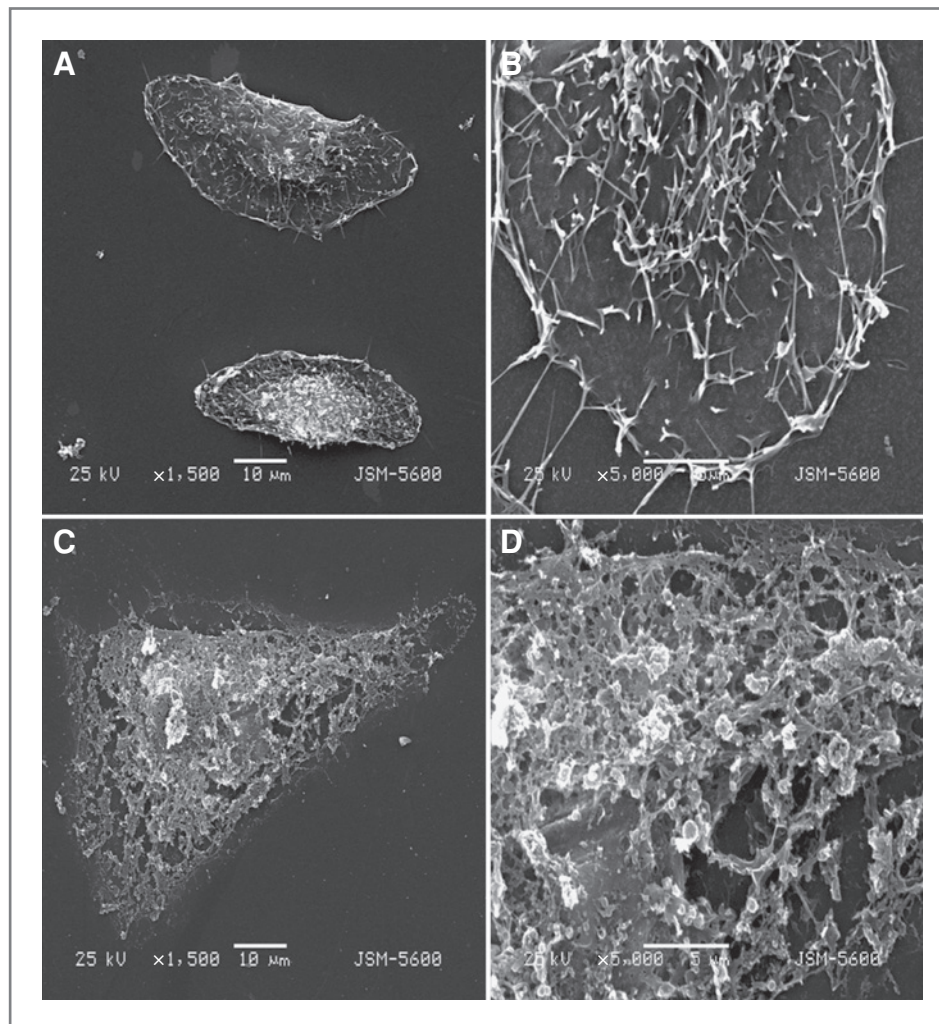


Figure 3. Effect of peptide A12L/A20L on the cell membrane of HeLa cells, using scanning electron microscopy. Untreated HeLa cells are shown in different magnifications in panels A and B. HeLa cells treated with peptide A12L/A20L for 1 hour revealed disrupted cell membranes in different magnifications in panels C and D.

Discussion

In this study, as shown in Fig. 4A, peptide hydrophobicity has a nonlinear correlation with the peptide helicity in 50% TFE ($R = 0.987$), which is a mimic of the hydrophobic environment of biomembrane. Increasing peptide hydrophobicity on the nonpolar face enhanced the helical structure for α -helical peptides. Hence, hydrophobicity is one of the critical factors for peptide secondary structure when peptides interact with the target cytoplasmic membrane.

Self-association ability may help peptide to aggregate with each other to form transmembrane pore or channel and cause the cell death. Peptide self-association ability showed a linear correlation with peptide helicity in solution ($R = 0.991$; Fig. 4B). This can be attributed to the fact that peptide with stronger helicity in solution usually exhibits more complete nonpolar face. Peptide self-association uses the nonpolar faces of peptide molecules to bind together by hydrophobic interaction. Thus, peptides showing higher helicity with fully

hydrophobic faces exhibited stronger self-association. Peptide self-association ability also exhibited effect on anticancer activity, that is, peptides with higher P_A values usually showed stronger anticancer activity (Tables 1 and 2).

In this study, we clearly show that the anticancer activity of the peptides was correlated with the peptide hydrophobicity (Table 2). Hydrophobicity also exhibited the similar trend of effects on hemolytic activity as on anticancer activity (Table 2). However, for the therapeutic index, the hydrophobicity showed different effects on peptide specificity against cancer cells and normal cells (Fig. 4C). At a relative low range of hydrophobicity, an increase in peptide hydrophobicity caused an increase in therapeutic index; in contrast, peptide therapeutic index was decreased with further increase in peptide hydrophobicity (Table 2; Fig. 4C). This can be explained by the significant increase of hemolytic activity at high hydrophobicity; hence, the specificity was low. For peptide specificity between cancer cells and normal cells, it is generally accepted that the specificity

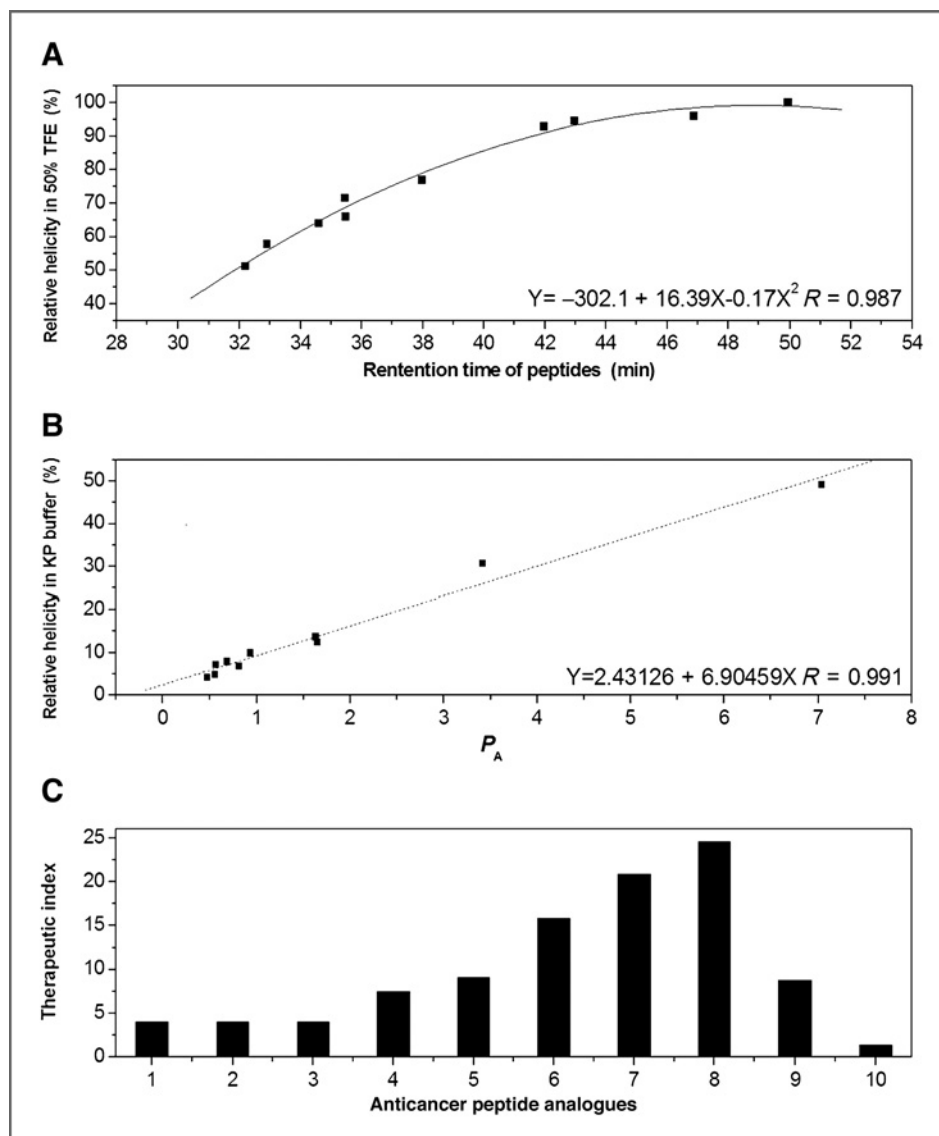


Figure 4. Relationships of peptide biophysical properties and biological activities. A, relationships of peptide hydrophobicity and helicity in hydrophobic environment; B, relationships of self-association ability and helicity in aqueous solution. The experimental data are from Table 1. Least-squares fit analysis showed correlations of $R = 0.987$ for peptide hydrophobicity and helicity in hydrophobic environment and $R = 0.991$ for self-association ability and helicity in aqueous environment. C, relationships of peptide hydrophobicity and specificity based on the data from Table 2. Peptides were in an increasing order of hydrophobicity from number 1 to 10 as numbered in Table 1.

depends on the compositional difference between the cell membranes (1). Many cancer cell membranes, in contrast to normal cell membranes characterized by zwitterionic phospholipids such as red blood cells, have more anionic phospholipids in their outer leaflet (3, 19, 20). In addition, many cancer cell membranes contain O-glycosylated mucin, a type of glycoprotein which increases additional negative charges on cancer cell surface (21). The stronger electrostatic interaction between cationic anticancer peptides and negatively charged cancer cell surface and membrane components contributes to the selectivity for cancer cells and healthy eukaryotic cells (1, 22). In addition, there is a higher number of microvilli on cancer cells than on normal cells (23), which results in the increase of membrane surface and enhances the concentration of bound peptide on cancer cell surface (3, 24).

The mode of cell death caused by anticancer peptides can be generally described as necrosis and/or apoptosis (1). For instance, Maher and colleagues recently reported that the anticancer peptide melittin exhibits necrotic cytotoxicity in gastrointestinal cells (8); however, the work of Moon and colleagues showed that the peptide melittin induces apoptosis in leukemic U937 cells (25). To understand the mechanism of action, we used FITC-labeled peptide localization, FITC–Annexin V/PI double staining, and electron scanning microscopic experiments to explore the mechanism of peptides killing cancer cells. The quick binding of peptide A12L/A20L on the surface of HeLa cells shows that the initial step of peptide–cell interaction is triggered by the strong electrostatic interaction, as illustrated by FITC-labeled peptide localization time study (Supplementary Fig. S2). It is clear to see that peptide A12L/A20L exhibited quick necrotic process

with lysis of the target HeLa membrane rather than apoptotic process in this study (Fig. 3). In our previous study, we proposed a membrane discrimination mechanism for α -helical antimicrobial peptides whose sole target is the biomembrane (26), based on a barrel-stave mechanism (27) in eukaryotic cells and a carpet mechanism (7) in prokaryotic cells. We believe that α -helical peptide forms pores or channels in eukaryotic cell membrane. The observation that there is a correlation between peptide hydrophobicity and anticancer/hemolytic activity is consistent with the membrane discrimination mechanism on eukaryotic cells. Peptides with higher hydrophobicity will penetrate deeper into the hydrophobic core of the cell membrane, causing stronger activity of forming pores or channels on cancer cell membrane, which may explain the reason that the higher hydrophobicity is always accompanied with the greater anticancer activity and hemolytic activity.

In summary, this study shows the important role of hydrophobicity in anticancer activity of the α -helical anticancer peptides. Peptides killed cancer cells with a fast necrotic mechanism causing cell membrane lysis as described in the membrane discrimination mechanism. In this study, utilizing *de novo* approach, we designed

anticancer peptides based on the secondary structure, showing much higher activity against cancer cells than traditional chemical drugs and good specificity between cancer cells and human normal cells. *De novo* peptide design approach proves its value of creating new anticancer therapeutics with promising potentials in clinical practice.

Disclosure of Potential Conflicts of Interest

No potential conflicts of interest were disclosed

Grant Support

This work was supported by Natural Science Foundation of China Grants 30940016 (Y. Chen) and 30971398 (Y. Liu), Grant for Doctorate Program of New Teacher, Ministry of Education of China 200801831064 (Y. Chen), Scientific Frontier and Interscience Innovation Program of Jilin University 200903095 (Y. Chen), Basic Scientific Research Grant of Jilin University (Y.B. Huang), and 985 Graduate Innovation Program of Jilin University 20080110 (X.F. Wang).

The costs of publication of this article were defrayed in part by the payment of page charges. This article must therefore be hereby marked *advertisement* in accordance with 18 U.S.C. Section 1734 solely to indicate this fact.

Received September 14, 2010; revised November 22, 2010; accepted December 6, 2010; published OnlineFirst January 20, 2011.

References

- Hoskin DW, Ramamoorthy A. Studies on anticancer activities of antimicrobial peptides. *Biochim Biophys Acta* 2008;1778:357–75.
- Dennison SR, Whittaker M, Harris F, Phoenix DA. Anticancer alpha-helical peptides and structure/function relationships underpinning their interactions with tumour cell membranes. *Curr Protein Pept Sci* 2006;7:487–99.
- Papo N, Shai Y. Host defense peptides as new weapons in cancer treatment. *Cell Mol Life Sci* 2005;62:784–90.
- Lee HS, Park CB, Kim JM, Jang SA, Park IY, Kim MS, et al. Mechanism of anticancer activity of buforin IIb, a histone H2A-derived peptide. *Cancer Lett* 2008;271:47–55.
- Papo N, Seger D, Makovitzki A, Kalchenko V, Eshhar Z, Degani H, et al. Inhibition of tumor growth and elimination of multiple metastases in human prostate and breast xenografts by systemic inoculation of a host defense-like lytic peptide. *Cancer Res* 2006; 66:5371–8.
- Ghavami S, Asoodeh A, Klonisch T, Halayko AJ, Kadkhoda K, Krocak TJ, et al. Brevinin-2R(1) semi-selectively kills cancer cells by a distinct mechanism, which involves the lysosomal-mitochondrial death pathway. *J Cell Mol Med* 2008;12:1005–22.
- Shai Y. Mechanism of the binding, insertion and destabilization of phospholipid bilayer membranes by alpha-helical antimicrobial and cell non-selective membrane-lytic peptides. *Biochim Biophys Acta* 1999;1462:55–70.
- Maher S, McClean S. Melittin exhibits necrotic cytotoxicity in gastrointestinal cells which is attenuated by cholesterol. *Biochem Pharmacol* 2008;75:1104–14.
- Chen Y, Mant CT, Farmer SW, Hancock RE, Vasil ML, Hodges RS. Rational design of alpha-helical antimicrobial peptides with enhanced activities and specificity/therapeutic index. *J Biol Chem* 2005; 280:12316–29.
- Huang JF, Xu YM, Hao DM, Huang YB, Liu Y, Chen YX. Structure guided *de novo* design of alpha-helical antimicrobial peptide with enhanced specificity. *Pure Appl Chem* 2010;82:243–57.
- Dewan PC, Anantharaman A, Chauhan VS, Sahal D. Antimicrobial action of prototypic amphiphatic cationic decapeptides and their branched dimers. *Biochemistry* 2009;48:5642–57.
- Mant CT, Chen Y, Hodges RS. Temperature profiling of polypeptides in reversed-phase liquid chromatography. I. Monitoring of dimerization and unfolding of amphiphatic alpha-helical peptides. *J Chromatogr A* 2003;1009:29–43.
- Lee DL, Mant CT, Hodges RS. A novel method to measure self-association of small amphiphatic molecules: temperature profiling in reversed-phase chromatography. *J Biol Chem* 2003;278:22918–27.
- Chen Y, Mant CT, Hodges RS. Determination of stereochemistry stability coefficients of amino acid side-chains in an amphiphatic alpha-helix. *J Pept Res* 2002;59:18–33.
- Zhou NE, Mant CT, Hodges RS. Effect of preferred binding domains on peptide retention behavior in reversed-phase chromatography: amphiphatic alpha-helices. *Pept Res* 1990;3:8–20.
- Kovacs JM, Mant CT, Hodges RS. Determination of intrinsic hydrophilicity/hydrophobicity of amino acid side-chains in peptides in the absence of nearest-neighbor or conformational effects. *Biopolymers (Peptide Sci)* 2006;84:283–97.
- Chen Y, Guarneri MT, Vasil AI, Vasil ML, Mant CT, Hodges RS. Role of peptide hydrophobicity in the mechanism of action of alpha-helical antimicrobial peptides. *Antimicrob Agents Chemother* 2007; 51:1398–406.
- Dolan JW. Temperature selectivity in reversed-phase high performance liquid chromatography. *J Chromatogr A* 2002;965:195–205.
- Papo N, Braunstein A, Eshhar Z, Shai Y. Suppression of human prostate tumor growth in mice by a cytolytic D-, L-amino Acid Peptide: membrane lysis, increased necrosis, and inhibition of prostate-specific antigen secretion. *Cancer Res* 2004;64:5779–86.
- Ran S, Downes A, Thorpe PE. Increased exposure of anionic phospholipids on the surface of tumor blood vessels. *Cancer Res* 2002;62:6132–40.
- Yoon WH, Park HD, Lim K, Hwang BD. Effect of O-glycosylated mucin on invasion and metastasis of HM7 human colon cancer cells. *Biochem Biophys Res Commun* 1996;222:694–9.
- Mader JS, Hoskin DW. Cationic antimicrobial peptides as novel cytotoxic agents for cancer treatment. *Expert Opin Investig Drugs* 2006;15:933–46.

23. Zwaal RF, Schroit AJ. Pathophysiologic implications of membrane phospholipid asymmetry in blood cells. *Blood* 1997;89:1121–32.
24. Chan SC, Hui L, Chen HM. Enhancement of the cytolytic effect of anti-bacterial cecropin by the microvilli of cancer cells. *Anticancer Res* 1998;18:4467–74.
25. Moon DO, Park SY, Choi YH, Kim ND, Lee C, Kim GY. Melittin induces Bcl-2 and caspase-3-dependent apoptosis through downregulation of Akt phosphorylation in human leukemic U937 cells. *Toxicon* 2008;51:112–20.
26. Chen Y, Vasil AI, Rehaume L, et al. Comparison of biophysical and biologic properties of α -helical enantiomeric antimicrobial peptides. *Chem Biol Drug Des* 2006;67:162–73.
27. Ehrenstein G, Lecar H. Electrically gated ionic channels in lipid bilayers. *Q Rev Biophys* 1977;10:1–34.